Dielectric and mechanoelastic relaxations due to point defects in layered bismuth titanate ceramics

2001 J. Phys.: Condens. Matter 13 7315

(http://iopscience.iop.org/0953-8984/13/33/312)

INSTITUTE OF PHYSICS PUBLISHING JOURNAL OF PHYSICS: CONDENSED MATTER

J. Phys.: Condens. Matter **13** (2001) 7315–7326 PII: S0953-8984(01)25448-4

Dielectric and mechanoelastic relaxations due to point defects in layered bismuth titanate ceramics

B Jiménez, R Jiménez, A Castro, P Millán and L Pardo

Instituto de Ciencia de Materiales de Madrid, CSIC, Cantoblanco, 28049 Madrid, Spain

E-mail: basilio.jimenez@icmm.csic.es

Received 4 June 2001, in final form 18 June 2001
Published 2 August 2001
Online at stacks.iop.org/JPhysCM/13/7315

Abstract

Complex permittivity and Young's modulus provide relevant information on the role of point defects in the dielectric and mechano-elastic properties of ferroelectric materials. Low-frequency measurements as a function of the temperature performed on $Bi_4Ti_3O_{12}$ (BIT) have shown that point and dipole defects are frozen close to domain walls. Low-temperature dipole defect relaxation processes take place with characteristic times (τ_0) of the order of 10^{-11} s and 10^{-12} s and activation energies (E_a) of 0.70 eV and 0.65 eV for dielectric and mechano-elastic relaxations, respectively. At higher temperatures new dielectric relaxation peaks appear that can be attributed to jumps of de-iced oxygen vacancies ($\tau_0 \cong 10^{-11}$ s, $E_a = 1.08$ eV, $T \cong 300\,^{\circ}$C) and to vacancy migration ($\tau_0 \cong 10^{-15}$ s, $E_a = 1.90$ eV, $T \cong 450\,^{\circ}$C). Elastic relaxation peaks are also present close to 300 °C whose activation energy (1.50 eV) and characteristic time (10^{-15} s) suggest a vacancy migration process. Close to 500 °C with $E_a = 2.30$ eV and $\tau_0 \cong 10^{-17}$ s another relaxation peak, which should correspond to domain wall viscous motion near the phase transition temperature, is observed. The Young's modulus has a smooth step at $T \cong 300\,^{\circ}$C that we attribute to a change in the mobility of oxygen vacancies with respect to the domain walls. Below 300 °C the vacancies are frozen in the domain walls and they are de-iced and distributed throughout the material at temperatures above 300 °C. The experimental results show that the material is softer when the vacancies are linked to domain walls than when they are distributed throughout the material. The diffusion of vacancies back to the domain wall traps at room temperature takes a long time (days).

1. Introduction

The ferroelectric compound $Bi_4Ti_3O_{12}$ is a member of the layered titanate (BIT) family [1], which are represented by the general formula $Bi_2A_{x-1}B_xO_{3x+3} = (Bi_2O_2)^{2+}(A_{x-1}B_xO_{3x+1})^{2-}$

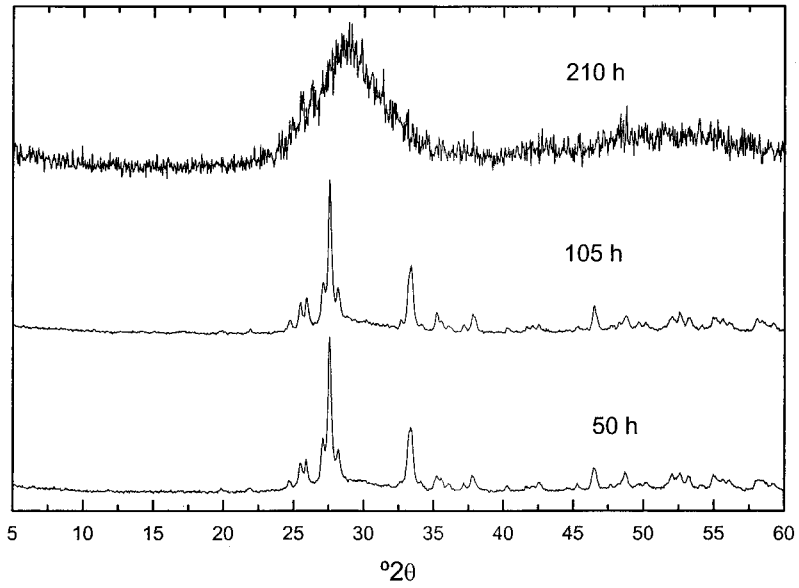

Figure 1. Milling time evolution of the x-ray diffraction pattern of the component oxide powders.

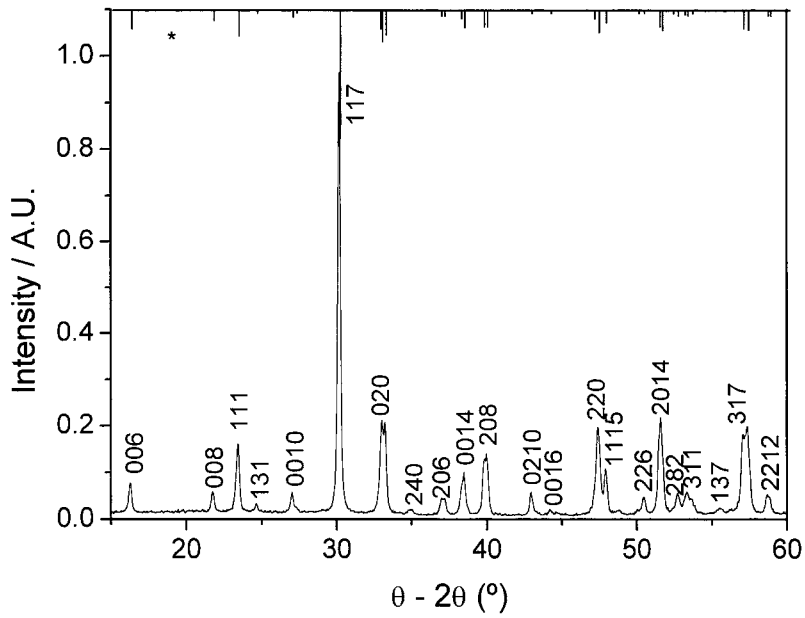

Figure 2. X-ray diffraction pattern of a BIT ceramic.

where A stands for a mono-, di- or trivalent ion, B is a transition metal cation such as Ti^{4+}, Nb^{5+} or Ta^{5+} and $x = 2$–4 is the number of perovskite layers sandwiched by two Bi_2O_2 layers.

The considerable interest in bismuth-layered compounds that has arisen in the last few years is due to their numerous applications in electronic devices [2, 3]. In this family, the BIT is a typical ferroelectric with a Curie temperature of 675 °C [4], which makes it useful

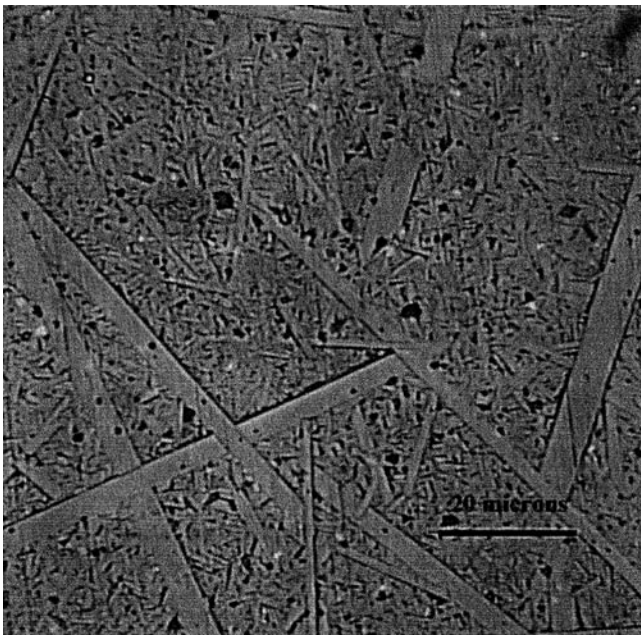

(a)

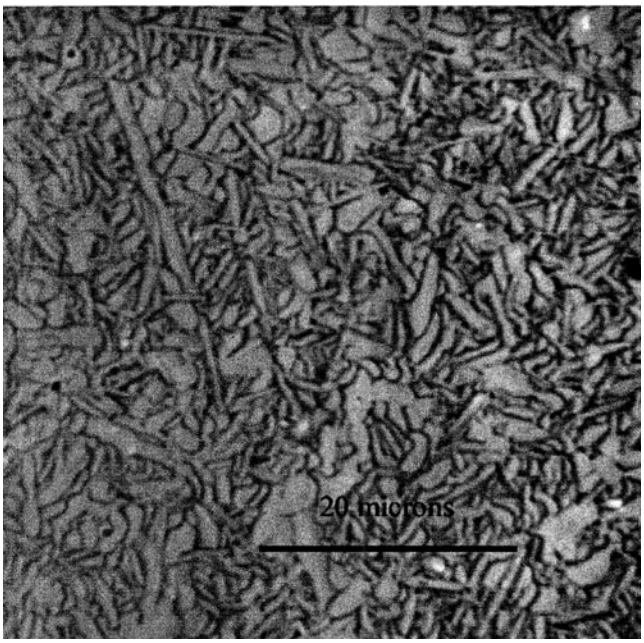

(b)

Figure 3. Optical micrographs of BIT ceramics: (a) normal sintering and (b) hot-pressing sintered.

for applications in a wide temperature range, prepared either as a bulk or thin-film material. This family also constitutes the background for creating new oxygen ion conductors with high conductivity at low temperature (600–800 °C) which are interesting as electrolytes for

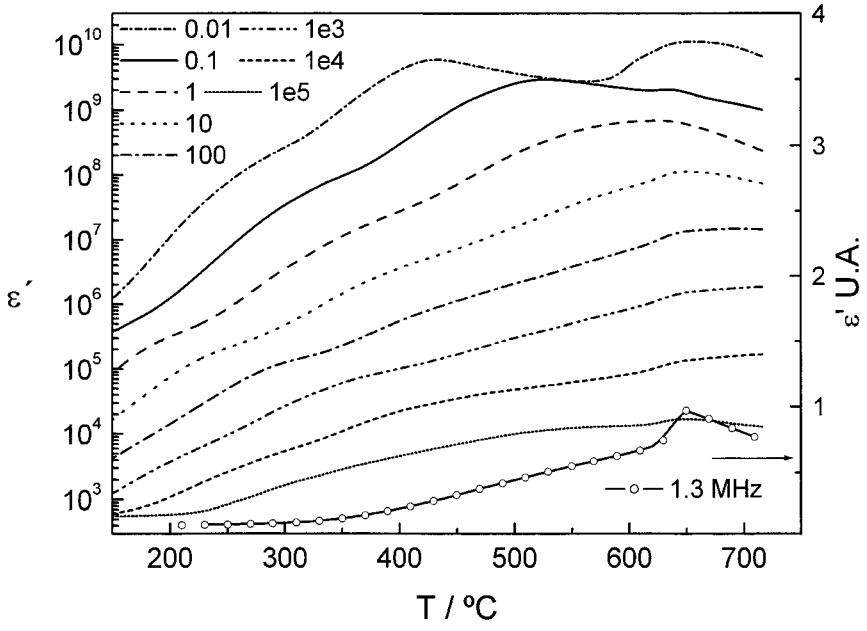

Figure 4. Dielectric constant as a function of temperature at different frequencies.

solid oxide fuel cell preparation and also shows structural similarities to high-temperature superconductors [5].

Much work has been carried out concerning the electrical and ferroelectric properties of BIT in the form of single crystals or polycrystals [6–8], where anomalies in some properties appear at temperatures below that of the phase transition. These anomalies, especially important in the low-frequency region $f < 10$ kHz, are attributed to different electrical charge contributions coming from jumping point defects such as oxygen vacancies or disordered cations [9].

Defects also affect the low-frequency mechano-elastic properties of ferroelectric materials due to the interaction between the domain walls and point defects that give rise to the relaxation peaks. Thus, a certain correlation with low-frequency dielectric properties, mainly between dielectric and mechanical losses, does exist [10, 11]. The aim of this work is to deliver information on the low-frequency elastic behaviour of BIT and on the influence and thermal evolution of charged point defects on both the dielectric and mechanical properties.

2. Experiment

$Bi_4Ti_3O_{12}$ was obtained from amorphous powders prepared by a mechano-chemical activation method [12]. Stoichiometric mixtures of analytical grade Bi_2O_3 and TiO_2 were homogenized by hand in an agate mortar and pestle for 3 min. The mechano-chemical activation was carried out on a Fritsch vibrating mill, model Pulverisette 0. The starting oxides mixture was placed in a stainless-steel pot with a 5 cm diameter steel ball and milled for various times between 1 and 210 h. The milling time evolution of the mixture x-ray diffraction patterns is shown in figure 1.

X-ray diffraction patterns were performed at room temperature with a Siemens Kristalloflex 810 computer-controlled diffractometer in the 5–70° (2θ) range, and a D 501

goniometer provided with a 2θ compensating slit and a graphite monochromator. Cu K_α ($\lambda = 1.5418$ Å) radiation was used in all experiments

The amorphous powders were shaped into thin pellets prepared under an isostatic pressure of 2000 kg cm^{-2}. Sintering was performed in air at temperatures of 945 °C or by hot-pressing at 875 °C and 250 kg cm^{-2}. Density values of 96% and 98% of the theoretical value were obtained for normal and hot-pressing sintering ceramics, respectively, by the Archimedes immersion method. The x-ray diffraction patterns of the ceramics give the BIT crystalline structure of an isotropic material, figure 2, according to 35-795 JCPDS-ICDD (c) 1992 powder data.

The microstructure of the ceramics obtained from the amorphous powder is depicted in figure 3. Figure 3(a), corresponding to the normal sintered ceramic, consists of needle shaped grains with high length/width ratio and some anomalous growth of very large grains. Figure 3(b) was obtained from the hot-pressing sintered ceramic and presents a smaller and more homogeneous grain size.

The dielectric permittivity as a function of the temperature and frequency was derived from impedance measurements performed with an HP4194A impedance analyser. In the frequency range 0.01–10^5 Hz we used a Solartron 1755 coupled with a potentiostat Parc 237A. For the low-frequency (0.1–30 Hz) elastic measurements as a function of the temperature the three point bending (TPB) method was used [13]. For TPB and impedance measurements, $11 \times 2 \times 0.1$ mm^3 samples and 11 mm diameter, 1.0 mm thick discs with sintered platinum paint on opposite faces, respectively, were used.

3. Experimental results

3.1. Dielectric behaviour

Dielectric measurements in BIT samples as a function of temperature in the range frequency 0.01 Hz–5 MHz were performed and non-outstanding qualitative differences were found for both kinds of ceramic. Figure 4 shows the results for the frequencies of 0.01 Hz–1.3 MHz. In the low-frequency range, we can observe undulations at temperatures of 250 and 450 °C that depend on the measuring frequency and wide peaks close to the phase transition temperature. These undulations move to higher temperatures when the measuring frequency increases. The peak in dielectric permittivity at the transition temperature is clearly observed at a frequency of 1.3 MHz. In the low-frequency region the peaks are masked by the effect of the universal dielectric response due to the low-frequency dispersion of non-free charge carriers and dielectric constant values are considerably increased.

The dielectric permittivity undulations become clear peaks in the thermal behaviour of the loss tangent, $\tan\delta_\varepsilon$: low-temperature peak P_0 in figure 5(a) and high-temperature peaks P_1 and P_2 in figure 5(b). In these figures the obtained results for frequencies from 0.01–100 kHz are plotted.

3.2. Elastic measurements

The Young's modulus, Y, and mechanical losses tangent, $\tan\delta_m$, as functions of the temperature for different frequencies of the dynamic mechanical stress of ceramic samples have been obtained. As the behaviour for all the measuring frequencies is qualitatively similar, in figure 6 we have plotted the results obtained for the frequency of 5 Hz.

We can distinguish three wide peaks, A_0, A_1 and A_2, in the loss tangent as well as the peak in the ferroelectric phase transition temperature. The temperatures of these peaks are in

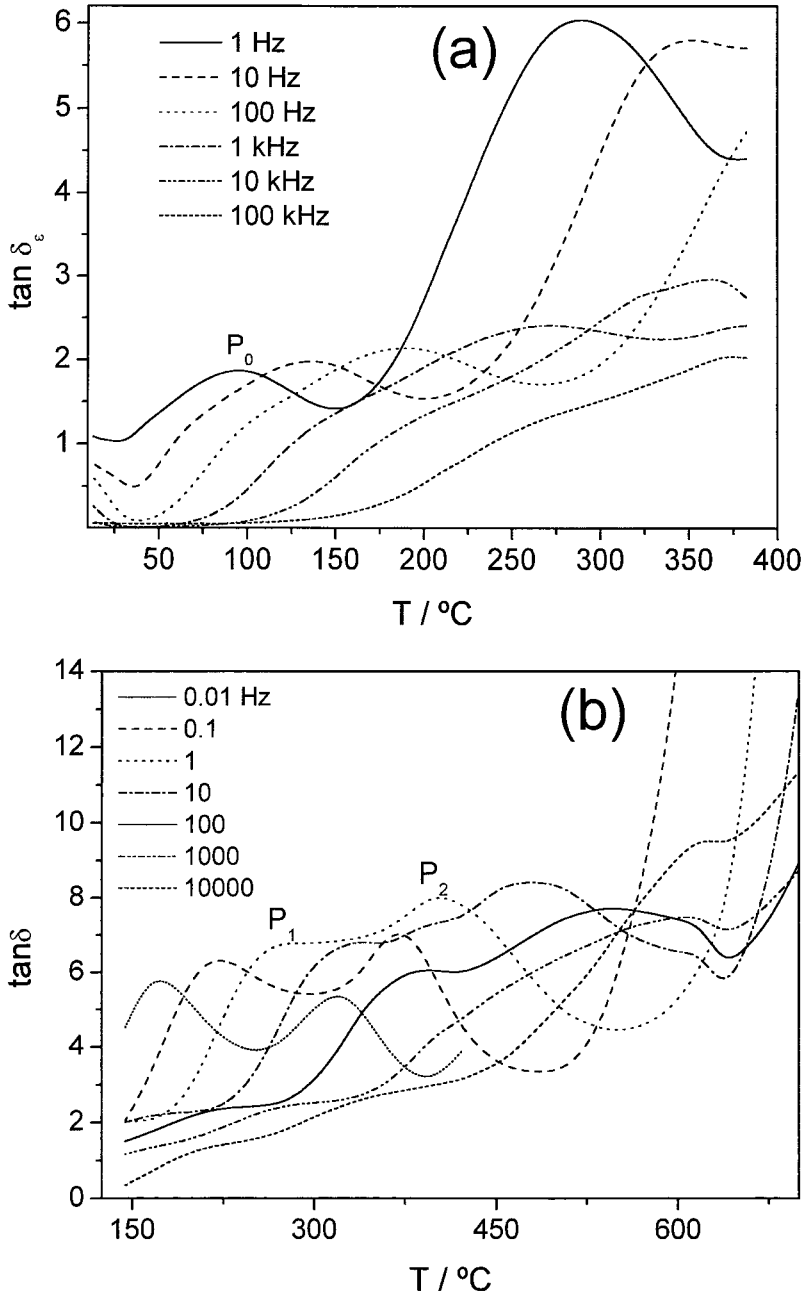

Figure 5. Dielectric loss tangent as a function of the temperature at different measuring frequencies: (a) in the low-temperature range and (b) in the high-temperature range.

the same temperature range as those of P_0, P_1 and P_2 in the dielectric losses. In all cases their temperatures increase with the increasing measuring frequency.

The Young's modulus, Y (figure 6), increases with the increase of temperature and shows steps at 300 °C, then decreases to a minimum at the phase transition temperature, $T_c = 665$ °C.

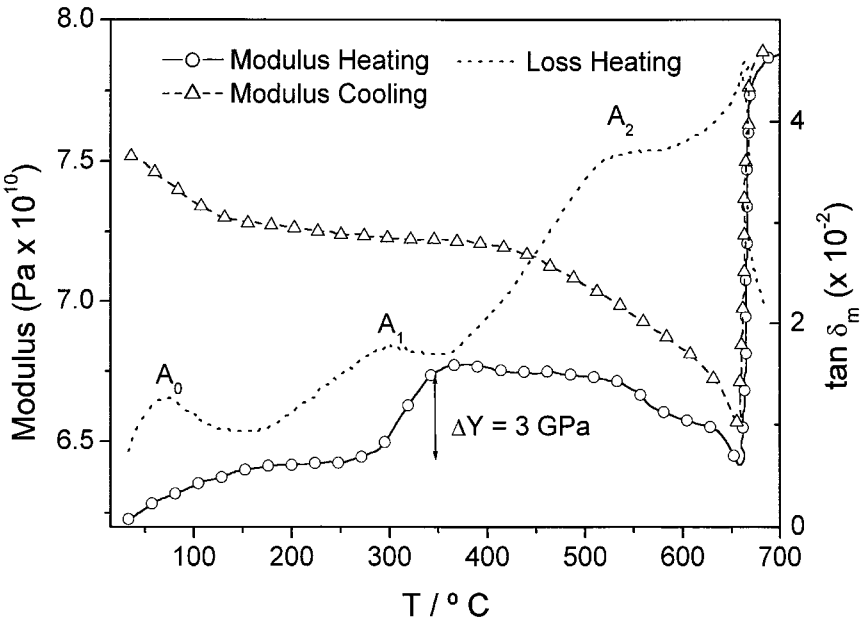

Figure 6. Young's modulus, Y, and mechanical loss tangent, tan δ_m, as functions of the temperature at 5 Hz dynamical stress.

In the cooling run the modulus presents a minimum in T_c, increases for some tens of degrees and then it maintains constant values until room temperature. Large differences in the modulus appear during the thermal cycle. Below the transition phase temperature, the modulus is much higher for the cooling run than that for the same temperature in the heating one and goes back to the original room-temperature value after a long time (days).

Around the phase transition temperature the Young's modulus behaves as in the case of perovskite-type ferroelectrics, PZT and PTCa, [13] where the Young's modulus decreases when the transition phase temperature is approximated from below and is clearly reversible in the complete thermal cycle.

4. Discussion

In figure 7, the Arrhenius plots obtained from the frequency and temperature of the maxima of dielectric (P_0, P_1, P_2) and mechanical (A_0, A_1, A_2) loss tangents are depicted. From these plots, and using the Arrhenius equation, we obtain the values for the activation energy and characteristic time that are shown in the table 1. As few points are available for the calculation of the activation energies from the mechanical loss tangent Arrhenius plots, an error in the obtained values of more than 10% must be considered

The activation energies of A_0 and P_0 are similar, but the characteristic time of A_0 is one order lower than that of P_0. It seems clear that these peaks correspond to the same relaxation mechanism and they could be correlated to the low-temperature dielectric loss tangent peak (I) obtained by Shulman *et al* ($E_a = 0.74$ eV, $\tau_0 = 1.1 \times 10^{-11}$ s) [9] that was attributed to dipole relaxation in a randomly oriented ceramic.

From dielectric measurements, the second peak, A_1, appears at temperatures very similar to those of peak P_1, but the activation energies and characteristic times are quite different (see

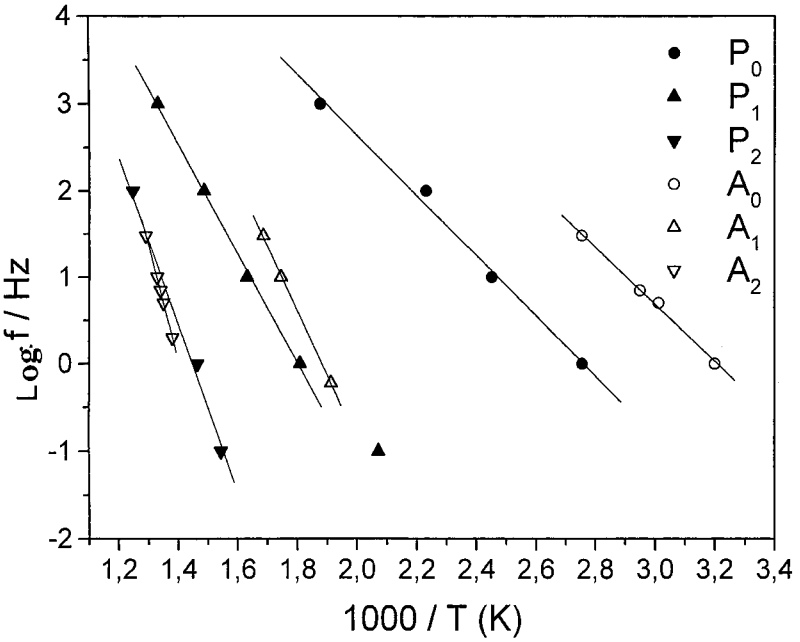

Figure 7. Arrhenius plots obtained from loss tangent peaks. The P's are from the dielectric loss tangent and the A's are from the mechanical loss tangent.

Table 1. Activation energies and characteristic times from: (P_i) dielectric, (A_i) elastic measurements.

Peak	E_a (eV)	τ_0 (s)
Dielectric		
P_0	0.70	5.0×10^{-11}
P_1	1.08	1.3×10^{-11}
P_2	1.90	2.0×10^{-15}
Mechano-elastic		
A_0	0.65	4.2×10^{-12}
A_1	1.50	1.6×10^{-15}
A_2	2.30	1.0×10^{-17}

table 1). The peak A_2 has a much higher activation energy and lower characteristic time than those of the peak P_2, but a similar peak temperature. The high values obtained for peak A_2 ($E_a = 2.3$ eV and $\tau_0 \cong 1.0 \times 10^{-17}$ s) are difficult to attribute to a dynamical relaxation process, it seems better to think of some kind of domain walls viscous movement [14]. The P_2 peak should better correspond to vacancy migration [15].

If the main point defect in layered ferroelectrics is concerned with oxygen vacancies and they are considered as being responsible for the observed relaxations, it is interesting to examine the possible movements of oxygen ions between positions in the structure (see figure 8).

According to Withers *et al* [16], the perovskite layer in the ferroelectric BIT contains eight almost-equivalent oxygen-ion positions [9], with a valence of -2.03 ± 0.03. Several possibilities can be envisioned for oxygen ions to switch positions with neighbouring vacant sites in the perovskite layer. The direction of many jumps, for example, O(1)–O(3)–O(1)′,

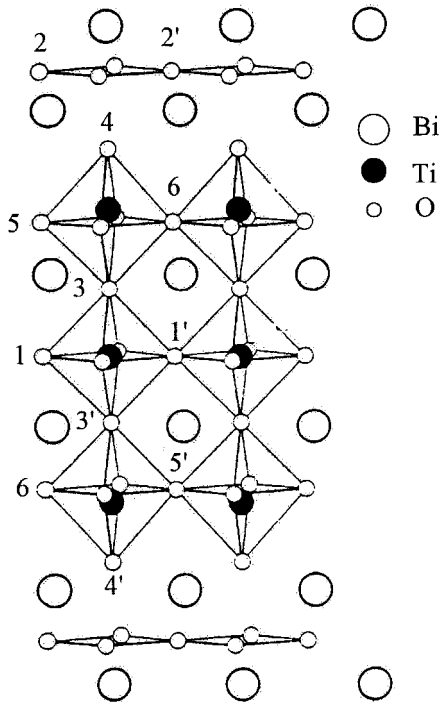

Figure 8. Projection on the *ab*-plane of the BIT parent structure. (After Whiters *et al* [14].)

would be 45° from the *a*- or *b*-directions. If this motion were responsible for the low-temperature relaxation, the relaxation would be observed in both the *c*-direction and the *ab*-plane, which was not the case.

By considering the oxygen-ion motion in the (Bi_2O_2) layer, they are either underbonded (O(2) and O(2′)) or overbonded (O(4) and O(4′)). The O(2) ion can move to three possible positions in the Bi_2O_2 layer: the O(2′), O(4) and O(4′) positions. The latter two are part of the perovskite layers. Only the O(2′) position has an almost equivalent charge, −2.30, compared to −2.36 for O(2). The direction of this jump lies exactly in the *ab*-plane and could be responsible of the low-temperature relaxation. X-ray photoelectron spectroscopy (XPS) studies [17] suggest that the oxygen vacancies are preferentially sited in the vicinity of the bismuth ions and, most probably, in those of the Bi_2O_2 layer.

Experimental results from Sinyakov *et al* [18] in single crystals and Shulman *et al* [9] in textured ceramics have shown that these mechanisms should be responsible for high- and low-temperature relaxations,

Vacancies can be present as individual, cluster or dipole M–V_o, [19] (M being Bi^{3+} or adsorbed oxygen ions) defects that accumulate and freeze close to or into domain walls and follow the low-frequency electric and elastic fields. Thus, the motion of different oxygen vacancy sites could explain the low- and high-temperature dielectric and elastic relaxations.

The isotropic character of our samples means that all the possible peaks can be present in the experimental results of dielectric measurements, as it really happens.

The dielectric characteristic time of the order of 10^{-11} s is typical of ionic jumps or dipole relaxation, therefore the peaks P_0 and P_1, with almost equal values for τ_0, should probably correspond to dipole defect relaxation and the jump of vacancies near the domain walls,

respectively. The lower temperature maximum, P_0, of the dielectric loss tangent should come from the relaxational behaviour of the dipole defect in the Bi_2O_2 layer. The second maximum, P_1, could be attributed to ionic jump between the equivalent variants. When the temperature increases, the third maximum, P_2, moves to higher temperatures with increasing frequency with an enormous increase in the dielectric constant, because the onset of vacancy migration should lead to universal dielectric behaviour producing this effect and also an increase in dielectric losses.

It is known [20] that the appearance of 90° domain walls and the internal stress fields created by the spontaneous strain below the ferro-paraelectric phase transition temperature influences the vacancy distribution in the vicinity of 90° domain walls. Defect clusters have been localized near domain walls in PZT [20]. More recently, Scott and Dawber [21] proposed that oxygen-vacancy planes that are pinning domain walls should be related to the fatigue mechanism in perovskite ferroelectrics.

Concerning the elastic behaviour, the clusters that are formed by the strong stress gradient existing in PZT compounds provoke a low-temperature relaxation process with activation energies of 0.60 eV and characteristic times of 2.6×10^{-9} s [14] and nonlinear elastic behaviour as in $SrTiO_3$ crystals [22]. On the other hand, the elastic thermal behaviour of the Aurivillius-type compound $SrBi_2Ta_2O_9$, (SBT), shows a low-temperature losses peak [14] with $E_a = 0.97$ eV and $\tau_0 = 1.0 \times 10^{-14}$ s that was attributed to the lattice relaxation of oxygen vacancies in the vicinity of 90° domain walls. In the case of SBT, where the existence of 90° domain walls is not clear [23], the spontaneous strain (0.005 nm for the Ta^{5+} ion) and the stress gradients are much lower than in PZT, the cluster formation is less probable because few vacancies can diffuse to possible 90° domain walls and the vacancies can move more easily. This small domain wall effect should support the existence of such a low value of the characteristic time τ_0 in this material at low temperature.

In the case of BIT, where the existence of some 90° domain walls was proposed [24], we obtain, for the low-temperature loss peak, values of 0.65 eV and times of 1.2×10^{-12} s for the activation energy and characteristic time, respectively. However, instead of classical 90° domain walls, the domain walls to be considered in this compound should be better related to the optically observed perpendicular arrangement of 180° domain walls [8], which should also be appropriate for charged point defect trapping and the existence of stresses. The activation energy value of 0.65 eV is quite similar to those of SBT and PZT, but the characteristic time is in the middle of those of PZT and SBT. This result could confirm the existence of some kind of 90° walls in BIT. Thus, the values obtained for the low-temperature relaxation peaks of the mechanical loss tangent can be explained through the above considerations.

The behaviour of the Young's modulus as a function of the temperature can also help us understand the roll of the point defects in the experimental results. The thermal behaviour of the Young's modulus shows large differences in the heating and cooling runs (see figure 6) on going up the phase transition temperature. This difference indicates that the point defects have suffered important modifications in their state when the material returns back to the ferroelectric phase from the paraelectric one.

In the heating run the modulus shows a smooth step close to 300 °C (peak A_1 of mechanical losses) that does not appear in the cooling run. When the transition temperature is approximated the modulus decreases until the phase transition temperature where the large jump of the modulus takes place. This behaviour below the phase transition temperature is very common in layered perovskite compounds [25].

We can assume that the frozen vacancies and pole defects start to move out of the domain walls at temperatures close to 300 °C and, consequently, the Young's modulus of the wall will increase, giving place to a step. At this temperature the defects de-ice from the domain

walls and migrate through the material. The defect distribution out of domain walls makes the material more stiff than in the case where they are in the domain walls. This assertion is based on the presence of the loss peak A_1 in both the heating and the cooling runs and the increase of the Young's modulus along the cooling run, where the oxygen vacancies and dipole defects have not yet diffused to the domain walls and are distributed over the material. They even spend days to diffuse to return to the situation they had before heating.

Modifications of the state of the defects in Aurivillius-type compounds such as SBN ($SrBi_2Nb_2O_9$) and BTN (Bi_3TiNbO_9) were revealed through EPR spectra [25], where almost-free electron lines appear after thermal treatment of the samples at 400 °C. This result should confirm the de-icing of point defects from domain walls in perovskite layered ferroelectrics and explain the behaviour of the complex Young's modulus that we found for BIT.

According to the experimental results (see figure 6) lower values of the Young's modulus below the phase transition temperature indicate that domain walls diminish the stiffness of the ferroelectric material. On the other hand, it is known that oxygen vacancies also produce mechanical softening [26]. Thus, we can understand the behaviour of the Young's modulus in the heating run by considering that the vacancies preferentially concentrate near the domain walls in individual or dipole defect form. They are frozen at room temperature, making the material mechanically softer. When the temperature increases, around 300 °C, the vacancies de-ice from domain walls and migrate, provoking hardening of the domain walls and the appearance of a step in the Young's modulus.

Taking into account the above considerations, we can define Y_{dw}, Y_{dw}^O as the Young's modulus of the domain walls and domain walls with frozen vacancies, respectively. We also define Y_d and Y_d^O as the Young's modulus corresponding to domains (vacancies in domain walls) and domains containing distributed vacancies, respectively. Then, if we take Y_1 as the Young's modulus when the domain walls contain frozen oxygen vacancies and Y_2 as the Young's modulus when the vacancies are distributed through the material and consider a series disposition between domains and domain walls, we have

$$\frac{1}{Y_1} = \frac{1}{Y_d} + \frac{1}{Y_{dw}^O}, \qquad \frac{1}{Y_2} = \frac{1}{Y_d^O} + \frac{1}{Y_{dw}}; \qquad \frac{1}{Y_1} - \frac{1}{Y_2} = \frac{1}{Y_{dw}^O} - \frac{1}{Y_{dw}} + \frac{1}{Y_d} - \frac{1}{Y_d^O}$$

$$\frac{\Delta Y}{Y_1 Y_2} = \frac{\Delta Y_{dw}}{Y_{dw} Y_{dw}^O} + \frac{\Delta Y_d}{Y_d Y_d^O}. \tag{1}$$

As the vacancies produce a softening of the modulus proportional to the vacancy concentration [24], we shall have $(Y_{dw})^O < (Y_{dw})$ and $Y_d^O \leqslant Y_d$ and $Y_d > Y_{dw}$. Then, we have

$$\Delta Y_{dw} = Y_{dw} - Y_{dw}^O > 0$$

and

$$\Delta Y_d = Y_d^O - Y_d < 0.$$

Then the sign of the second term of the second member of (1) is negative and its absolute value will be lower than that of the first term. Thus, the step close to 300 °C in the modulus should be positive, in accordance with the experimental results.

5. Conclusions

Dielectric and mechano-elastic measurements have shown that point defects and their relation with ferroelectric domain walls are responsible for the relaxations appearing in the dielectric and elastic loss tangents at low frequencies over a wide range of temperature.

Low-temperature peaks are attributed to the dipole defect frozen inside or close to domain walls, whose relaxation processes have characteristic times of 10^{-11} s and 10^{-12} s—for dielectric and mechano-elastic relaxations, respectively.

Peaks, which characteristic times are of the order of 10^{-15} s are most likely due to oxygen vacancy movement out (migration) of domain walls, and took place at higher temperatures ($\geqslant$300 °C).

The large difference in the value of the Young's modulus in the heating and cooling runs can be attributed to the fact that the oxygen vacancies are located in or close to the domain walls (heating run) or out of domain walls (cooling run). In the heating run the material is softer than in the cooling run. The recovery of the initial value takes a very long time (days).

The step near 300 °C in the Young's modulus is due to the de-icing of the oxygen vacancies from domain walls and their distribution throughout the material.

Acknowledgment

This work was supported by Spanish CICYT, project MAT97-0711.

References

[1] Aurivillius B 1949 *Ark. Kemi.* **1** 463
[2] Takenaka T and Sakata K 1984 *J. Appl. Phys.* **55** 1092
[3] Scott J F and Paz de Araujo C A 1989 *Science* **246** 1400
[4] Fouskova A and Cross L E 1970 *J. Appl. Phys.* **41** 3834
[5] Postnikov A V, Bartkovski St, Mersch F and Neuman M 1995 *Phys. Rev.* B **52** 805
[6] Jiang A Q and Zhang L D 1999 *Phys. Rev.* B **60** 9204
[7] Ehara S, Muramatsu K, Shimazu M, Tanaka J, Mori Y, Hattori T and Tamura H 1981 *Japan. J. Appl. Phys.* **20** 877
[8] Irie H, Miyayama M and Kudo T 1999 *Japan. J. Appl. Phys.* **38** 5958
[9] Shulman H S, Damjanovic D and Setter N 2000 *J. Am. Ceram. Soc.* **83** 528
[10] Chen Ang, Scott J F, Zhi Yu, Ledbetter H and Baptista J L 1999 *Phys. Rev.* B **59** 6661
[11] Hardtl K H 1982 *Ceram. Int.* **8** 121
[12] Castro A, Millán P, Pardo L and Jiménez B 1999 *J. Mater. Chem.* **9** 1313
[13] Jiménez B and Vicente J M 1998 *J. Phys. D: Appl. Phys.* **31** 130
[14] Wang Zhi Yong, Chen Ting-guo, Zhu Wei-min, Fu Jian, Yang Hai-Xue and Li Chen-en 1998 *Acta Phys. Sinica* **7** 764
[15] Schaefer H E, Damson B, Weller M, Arzt E and George E P 1997 *Phys. Status Solidi* a **160** 531
[16] Withers R L, Thompson J G and Rae A D 1991 *J. Solid State Chem.* **94** 404
[17] Jovalekic' C, Pavlovic' M, Osmokrovic' P and Atanasoka Lj 1998 *Appl. Phys. Lett.* **72** 1051
[18] Sinyakov E V, Dudnik E F, Duda V M, Podol'ski V A and Gorfunkel M A 1974 *Sov. Phys.–Solid State* **16** 979
[19] Jiang A Q, Hu Z X and Zhang L D 1999 *Appl. Phys. Lett.* **74** 114
[20] Arlt G 1990 *J. Mater. Sci.* **25** 2655
[21] Scott J F and Dawber M 2000 *Appl. Phys. Lett.* **76** 3801
[22] Kityk A V, Salje E K H and Scott J F 2000 *Phys. Rev.* B **61** 946
[23] Newnham R E, Wolfe W and Dorrian J F 1971 *Mater. Res. Bull.* **6** 1029
[24] Nistor L, Van Tendeloo G and Amelinckx S 1996 *Phase Transitions* **59** 135
[25] Jiménez B, Duran-Martín P, Jiménez-Rioboo R J and Jiménez R 2000 *J. Phys.: Condens. Matter* **12** 3883
[26] Grimwall G 1986 *Thermophysical Properties of Materials* vol XVIII, ed E P Wohlfarth (Amsterdam: North-Holland) ch 3, p 58